Werk

Jahr: 1978
Kollektion: fid.geo
Signatur: 8 Z NAT 2148:45
Digitalisiert: Niedersächsische Staats- und Universitätsbibliothek Göttingen
Werk Id: PPN1015067948_0045
PURL: http://resolver.sub.uni-goettingen.de/purl?PPN1015067948_0045

LOG Id: LOG_0030
LOG Titel: Theoretical investigations on acoustic remote sensing of ocean surface waves
LOG Typ: article

Übergeordnetes Werk

Werk Id: PPN1015067948
PURL: http://resolver.sub.uni-goettingen.de/purl?PPN1015067948
OPAC: http://opac.sub.uni-goettingen.de/DB=1/PPN?PPN=1015067948

Contact

Niedersächsische Staats- und Universitätsbibliothek Göttingen
Georg-August-Universität Göttingen
Platz der Göttinger Sieben 1
37073 Göttingen
Germany
Email: gdz@sub.uni-goettingen.de

J. Geophys. 45, 183–198, 1979

Journal of Geophysics

Theoretical Investigations on Acoustic Remote Sensing of Ocean Surface Waves

H.-H. Essen

Institut für Geophysik, Universität Hamburg,
D-2000 Hamburg 13, Bundesstraße 55, Federal Republic of Germany

Abstract. Some aspects of acoustic remote sensing in the ocean are discussed with application to surface waves. Bragg scattering is assumed for the physical mechanism of modulating the acoustic carrier. The frequencies necessary for that mechanism are in the range of some 100 Hz. It is shown that the variance spectrum of the modulated slowly varying acoustic amplitude is the appropriate quantity for deriving the relevant statistical properties of surface waves. For remote sensing the relationship between the measured acoustic and unknown surface-wave spectrum is described by a transfer function. Theoretical transfer functions are computed for CW (continuous wave) measurements over long ranges in shallow water. A mode- and a ray-propagation model are considered and the numerical results are compared. The transfer function depends strongly on the angular distribution of surface waves, which usually is unknown. If, on the other hand, both the 1-dimensional acoustic and waveheight spectrum are measured simultaneously these values can be used to determine the angular-distribution function. The necessary assumptions for this method are discussed and a simple model is presented which allows the application of matrix inversion.

Key words: Underwater acoustic – Remote sensing – Ocean-surface waves.

1. Introduction

In the last ten years the interest of oceanographers in remote-sensing methods has increased. Especially the technique of radar backscatter from the rough sea surface has been developed. The mechanism involved is Bragg scattering which presumes a matching of radio wavelengths to surface wavelengths. For example, HF radio waves are scattered by long ocean waves and the backscattered signal yields information on the 2-dimensional wave-height spectrum as well as near-surface currents (Tyler et al., 1974; Barrick et al., 1977).

0340-062X/79/0045/0183/$03.20

Due to the strong attenuation of radio waves within sea water only acoustic waves are appropriate for remote sensing of the inner ocean. A possible mechanism of coupling oceanic motions to acoustic waves is again Bragg scattering. Considering e.g. the problem of measuring surface waves by means of sound scattering the wavelength matching then requires low acoustic frequencies.

Contrary to the radar technique forward scattering is considered, i.e., source and receiver are at separate positions. Due to the long duration of acoustic echos, especially in shallow water, backscatter methods are not applicable.

In the present paper results of theoretical investigations on acoustic remote sensing in the ocean are reported. The acoustic measurement system consists of a bottom-mounted source and a receiver. A low-frequency continuous wave (CW) is transmitted over a fixed range in the ocean and is modulated in amplitude and phase by the water motions. Observations show that the modulation frequencies correspond to the frequencies of oceanic motions, e.g. surface waves, internal waves, tides, etc. (Clark and Kronengold, 1974; Essen et al., 1978). While the first cited paper considers the influence of long-period motions, the second one investigates the remote sensing of surface waves, which also is the topic of the following chapters.

In Chapter 2 the theory of acoustic scattering from a rough sea surface is outlined in the limit of Bragg scattering. The surface-wave heights are random variables and thus the Doppler-shifted portion of the received signal is random as well. This aspect is considered in Chapter 3. An acoustic spectrum is defined which may be related to the variance spectrum of surface wave heights by a transfer function. The transfer function itself depends on the geometry of the acoustic propagation. For shallow water and low frequencies the sound field is best represented by normal modes. In Chapter 4 numerical results for the transfer function are shown where both mode- and ray-models are used. It turns out that the results become the same if the number of trapped modes is 8 or more.

A further result is that the transfer function strongly depends on the angular distribution of surface waves. This undesired property for the determination of the 1-dimensional wave-height spectrum from acoustic measurements may be used on the other hand for estimating the angular distribution. For this purpose both the acoustic and the 1-dimensional wave height spectrum must be measured and it has to be assumed that the angular distribution function does not depend on frequency, at least within a certain interval. In Chapter 5 a technique is presented to compute the surface-wave angular distribution from the measured transfer function by a matrix inversion.

2. Scattering Mechanism

The influence of the sea surface is treated in the limit of weak wave-wave interaction, or Bragg scattering. The rough surface may be compared with a moving grate. Considering an incoming plane acoustic wave the outgoing field includes a number of scattered Doppler-shifted waves beside the specular reflected one. The technique for handling this problem mathematically is perturbation expansion, which will be briefly outlined according to Essen (1974).

The sea surface may be described by the temporally varying deviations from a mean plane ($x_3=0$),

$$x_3=\zeta(x_1, x_2, t) \tag{1}$$

which are suitably presented by a Fourier sum of plane waves,

$$\zeta=\sum_{\boldsymbol{\kappa}} Z_{\boldsymbol{\kappa}} \exp\{i(\boldsymbol{\kappa}\boldsymbol{x}-\sigma t)\}+\text{c.c.} \tag{2}$$

$Z_{\boldsymbol{\kappa}}$ = complex Fourier amplitude
$\boldsymbol{\kappa}=(\kappa_1, \kappa_2)$ = horizontal wavenumber vector
σ = circular frequency

Since a real notation is needed for later computations the complex conjugated solution (c.c.) is added. Within this paper the validity of the deep-water dispersion relation is assumed,

$$\sigma^2=g\kappa. \tag{3}$$

The boundary condition for a sound wave at a pressure-free surface is,

$$p=0 \quad \text{at} \quad x_3=\zeta \tag{4}$$

and a Taylor expansion at the undisturbed surface yields,

$$p+\frac{\partial p}{\partial x_3}\cdot\zeta+---=0 \quad \text{at} \quad x_3=0. \tag{5}$$

Acoustic propagation may be presented by modes or rays. In both cases the scattered sound field is obtained from a perturbation expansion,

$$p=p^{(1)}+p^{(2)}+--- \tag{6}$$

with,

$$|p^{(1)}|\gg|p^{(2)}|\gg---.$$

From Eqs. (5)–(6) the boundary conditions of 1. and 2. order become,

$$p^{(1)}=0 \quad \text{at} \quad x_3=0 \tag{7}$$

$$p^{(2)}=-\frac{\partial p^{(1)}}{\partial x_3}\cdot\zeta \quad \text{at} \quad x_3=0 \tag{8}$$

where formally ζ is of 1. perturbation order.

Inhomogeneities within the water may be neglected and the wave equation is undisturbed in all perturbation orders,

$$\frac{\partial^2 p^{(l)}}{\partial t^2}-c_W^2\frac{\partial^2 p^{(l)}}{\partial x_i\,\partial x_i}=0 \qquad (i=1, 2, 3) \tag{9}$$

with, $l=1, 2, \ldots$, and, c_W = sound velocity of water.

The first-order plane-wave solution satisfying the wave equation and the boundary condition is,

$$p^{(1)} = P_0 \exp\{i(\boldsymbol{k}\boldsymbol{x} + k_3 x_3 - \omega_0 t)\} + \text{c.c.} \\ - P_0 \exp\{i(\boldsymbol{k}\boldsymbol{x} - k_3 x_3 - \omega_0 t)\} + \text{c.c.} \tag{10}$$

$$\boldsymbol{k} = (k_1, k_2), \quad k_3 = \sqrt{\frac{\omega_0^2}{c_W^2} - k^2} = \text{ wave number of the incident plane wave}$$

$$\frac{\omega_0}{2\pi} = \text{ source frequency.}$$

This solution includes the incident and the specular reflected wave. By inserting (2) and (10), the second order boundary condition (8) and the wave Eq. (9) yield the solution,

$$p^{(2)} = -2i \sum_{\substack{\boldsymbol{\kappa} \\ s = \pm 1}} k_3 P_0 Z_{\boldsymbol{\kappa}}^s \exp\{i(\boldsymbol{k}_s \boldsymbol{x} + k_{s3} x_3 - (\omega_0 + s\sigma) t\} + \text{c.c.} \tag{11}$$

$$Z_{\boldsymbol{\kappa}}^+ = Z_{\boldsymbol{\kappa}}, \quad Z_{\boldsymbol{\kappa}}^- = Z_{\boldsymbol{\kappa}}^*$$

$$\boldsymbol{k}_s = \boldsymbol{k} + s\boldsymbol{\kappa}, \quad k_{s3} \approx \sqrt{\frac{\omega_0^2}{c_W^2} - k_s^2} \quad (\text{as } \sigma \ll \omega_0).$$

Apparently, each Fourier component $\boldsymbol{\kappa}$ of the surface-wave field produces two scattered acoustic waves which are Doppler-shifted by $\pm\sigma$ from the carrier frequency ω_0.

The perturbation condition (2.6) requires,

$$k_3 |\zeta| \ll 1. \tag{12}$$

Considering a 200 Hz acoustic wave at 45° incidence angle one obtains for 1 m peak-to-trough wave height, $k_3 |\zeta| \approx 0.2$. This example illustrates the validity of the theory.

3. Continuous-Wave (CW) Source and Fixed-Range Propagation

If the theoretical considerations about scattering are applied to acoustic measurements in the ocean, the experimental configuration and the random nature of surface waves must be considered. In this paper we will refer to measurements carried out with a low-frequency source, where a CW signal is transmitted over a fixed range in the ocean. Usually source and receiver are placed at the bottom of the sea. Due to water motions the acoustic pressure is modulated in amplitude and phase,

$$p(t) = A(t)\cos[\omega_0 t - \Phi(t)]$$
$$= X(t)\cos(\omega_0 t) + Y(t)\sin(\omega_0 t) \tag{13}$$

with,

$$X(t) = A(t)\cos\Phi(t), \qquad Y(t) = A(t)\sin\Phi(t).$$

Following the Bragg-scattering theory the received signal consists of a superposition of first order coherent and second order Doppler-shifted waves. Beside these contributions the oceanic noise must be included,

$$p(t) = p_0(t) + p_s(t) + p_N(t). \tag{14}$$

The coherent portion may be written as,

$$p_0(t) = A_0(t)\cos(\omega_0 t - \Phi_0) \tag{15}$$

with,

$A_0, \Phi_0 =$ constant.

The contribution from scattered waves is modulated in amplitude and phase by the motion of surface waves.

$$p_s(t) = A_s(t)\cos[\omega_0 t - \Phi_s(t)]$$
$$= X_s(t)\cos(\omega_0 t) + Y_s(t)\sin(\omega_0 t). \tag{16}$$

Due to the randomness of surface waves p_s is a random variable. To a good approximation the surface waveheight ζ is a homogeneous, stationary Gaussian process. Thus the Fourier coefficients $Z_{\boldsymbol{\kappa}}$ in (2) are independent Gaussian variables with, cf. Kinsman (1965)

$$\langle Z_{\boldsymbol{\kappa}} \rangle = 0$$
$$\langle Z_{\boldsymbol{\kappa}} Z_{\boldsymbol{\kappa}'} \rangle = 0, \qquad \langle Z_{\boldsymbol{\kappa}} Z^*_{\boldsymbol{\kappa}'} \rangle = 0 \quad \text{if} \quad \boldsymbol{\kappa} \neq \boldsymbol{\kappa}' \tag{17}$$

and,

$$\langle \zeta^2 \rangle = 2\sum_{\boldsymbol{\kappa}} \langle |Z_{\boldsymbol{\kappa}}|^2 \rangle = \iint E_G(\boldsymbol{\kappa})\, d\boldsymbol{\kappa}.$$

The cornered parentheses denote ensemble-mean values. Considering now the second-order solution (11) the single components of the scattered field turn out to be proportional to the Gaussian variable $Z_{\boldsymbol{\kappa}}$. Decomposing the components into $\cos(\omega_0 t)$- and $\sin(\omega_0 t)$-portions, these are uncorrelated as a result of (17). The received acoustic signal is a superposition of all scattered wave components reaching the hydrophone from different directions. Thus if ζ is a zero-mean Gaussian variable it follows that X_s and Y_s are uncorrelated zero-mean Gaussian variables with equal variance,

$$\langle X_s \rangle = \langle Y_s \rangle = 0, \qquad \langle X_s Y_s \rangle = 0$$
$$\langle X_s^2 \rangle = \langle Y_s^2 \rangle = \int F_s(\sigma)\, d\sigma. \tag{18}$$

$F_s(\sigma) =$ variance spectrum of scattered waves.

Here the circular frequency is denoted by σ in order to distinguish the low oceanic frequencies (σ) from the high acoustic frequencies (ω).

Before recording the received signal on tape it is filtered by a small bandpass centered at the carrier frequency ω_0. Due to the Fourier expansion,

$$p_N(t)=\sum_{n=1}^{\infty}\{\alpha_n\cos(\omega_n t)+\beta_n\sin(\omega_n t)\} \tag{19}$$

the noise contribution may be written

$$p_N(t)=X_N(t)\cos(\omega_0 t)+Y_N(t)\sin(\omega_0 t) \tag{20}$$

with,

$$X_N(t)=\sum_{n=1}^{\infty}\{\alpha_n\cos[(\omega_n-\omega_0)t]+\beta_n\sin[(\omega_n-\omega_0)t]\},$$

$$Y_N(t)=\sum_{n=1}^{\infty}\{\beta_n\cos[(\omega_n-\omega_0)t]-\alpha_n\sin[(\omega_n-\omega_0)t]\}.$$

It should be pointed out that, as a result of bandpass filtering, $X_N(t)$ and $Y_N(t)$ are slowly varying as compared with the carrier signal. Furthermore it may be shown [cf. Rice (1954)] that if $p_N(t)$ is a Gaussian process with zero mean then $X_N(t)$ and $Y_N(t)$ are uncorrelated zero-mean Gaussian processes with equal variance,

$$\begin{aligned}&\langle X_N\rangle=\langle Y_N\rangle=0, \quad \langle X_N\,Y_N\rangle=0\\ &\langle X_N^2\rangle=\langle Y_N^2\rangle=\int F_N(\sigma)\,d\sigma\end{aligned} \tag{21}$$

with,

$$\sigma=\omega-\omega_0.$$

For our investigations only the variance spectra of $X_s(t)$ and $Y_s(t)$ from the scattered acoustic waves are of interest. In order to compute these spectra the received (bandpass-filtered) signal is demodulated by multiplying with $\cos(\omega_0 t)$ or $\sin(\omega_0 t)$ and by averaging over an acoustic period. On the basis of (14)–(16) and (19) one obtains,

$$\begin{aligned}X(t)&=2\overline{p(t)\cos(\omega_0 t)}=A_0\cos\Phi_0+X_s(t)+X_N(t)\\ Y(t)&=2\overline{p(t)\sin(\omega_0 t)}=A_0\sin\Phi_0+Y_s(t)+Y_N(t).\end{aligned} \tag{22}$$

This result implies that $X_{S,N}(t)$ and $Y_{S,N}(t)$ are slowly varying during an acoustic period.

For surface waves only frequencies up to 0.5 Hz are considered here, which correspond to a frequency band of $(\omega_0/2\pi\pm 0.5)$ Hz. Within this small band the noise may be assumed to be white,

$$F_N(\sigma)=\text{const.} \tag{23}$$

For convenience the acoustic spectrum is defined by,

$$\tfrac{1}{2}(\langle X^2\rangle + \langle Y^2\rangle) = \int F_A(\sigma)\, d\sigma. \tag{24}$$

It may be expected that the scattered acoustic signal is uncorrelated with oceanic noise. Therefore $F_A(\sigma)$ defined by (24) becomes, cf. (18), (21), and (22),

$$F_A(\sigma) = \tfrac{1}{2}A_0^2\, \delta(\sigma) + F_S(\sigma) + F_N(\sigma). \tag{25}$$

The coherent waves only contribute at zero frequency. The contribution of noise may be estimated by the frequency-independent portions within the observed spectra.

4. Transfer Functions

The acoustic measurements yield the 1-dimensional variance spectrum $F_A(\sigma)$ as defined by (24). For describing the ocean surface a 2-dimensional spectrum is needed, such as the directional waveheight spectrum $E_G(\boldsymbol{\kappa})$ introduced by (17). The aim now is to derive the relation between these spectra. Considering only second-order scattered waves it may be concluded from the foregoing considerations that a surface wave of frequency σ yields a contribution to the scattered variance spectrum $F_S(\sigma)$ at the same frequency. Thus the desired relation will be,

$$F_s(\sigma) = \int \tilde{T}(\sigma, \alpha)\, \tilde{E}_G(\sigma, \alpha)\, d\alpha \tag{26}$$

with,

$$\boldsymbol{\kappa} = (\kappa \cos\alpha,\ \kappa \sin\alpha).$$

$$\tilde{E}_G(\sigma, \alpha) = \kappa \frac{d\kappa}{d\sigma} E_G(\boldsymbol{\kappa}).$$

For comparing the measured spectrum $F_A(\sigma)$ with the theoretical $F_S(\sigma)$ the noise contribution must be estimated, cf. (25).

The directional dependence of surface waves can be separated from the 2-dimensional spectrum according to,

$$\tilde{E}_G(\sigma, \alpha) = F_G(\sigma) \cdot S_G(\sigma, \alpha) \tag{27}$$

where

$$\int_{-\pi}^{\pi} S_G(\sigma, \alpha)\, d\alpha = 1.$$

Inserting (27) into (26) one obtains,

$$F_S(\sigma) = T(\sigma) \cdot F_G(\sigma) \tag{28}$$

with,

$$T(\sigma) = \int_{-\pi}^{\pi} \tilde{T}(\sigma, \alpha)\, S_G(\sigma, \alpha)\, d\alpha.$$

With this equation the inversion, that is the determination of the surface-waveheight spectrum from the measured acoustic spectrum becomes trivial, as $T(\sigma)$ is known from theory. On the other hand, only the 1-dimensional frequency spectrum may be estimated, and no information is obtained on the directional distribution of surface waves. The angular distribution function $S_G(\sigma, \alpha)$ must be even known for computing the transfer function $T(\sigma)$. This restriction will be discussed again at the end of this chapter.

The transfer function will now be computed for long-range propagation, which means that the distance between source and receiver is assumed to be large compared to the water depth, and that the sound waves undergo many bounces at the sea surface and the bottom.

Sound propagation can be described by modes or rays. For low-frequency shallow-water propagation the mode representation is more appropriate. We will consider both, modes and rays, and compare the computed transfer functions.

Mode Propagation

We assume a water layer of constant depth overlying a homogeneous sedimentary halfspace, which may be treated as a fluid. This simple model has been shown to yield good agreement between computed and observed mode characteristics such as depth dependence of the amplitudes and group velocities of the single modes.

The first-order acoustic wave field is generated by a CW point source located at $(r=0, x_3=d)$ within the water layer, cf. Fig. 1. Thus the wave equation within first order becomes,

$$\frac{1}{c_W^2}\frac{\partial^2 p^{(1)}}{\partial t^2}-\frac{\partial^2 p^{(1)}}{\partial x_i\,\partial x_i}=Q\,\delta(x_1)\,\delta(x_2)\,\delta(x_3-d)\cos(\omega_0 t) \tag{29}$$

where $Q=$source strength,
while the second-order Eq. (9) remains unchanged. Additional to the boundary conditions (7), (8) at the surface and to the wave Eqs. (9) or (29) the boundary conditions at the sea floor and the wave equation within the sedimentary halfspace must be considered. They are undisturbed in all perturbation orders.

At a fluid-fluid interface continuity of pressure and of the normal component of particle velocity are required,

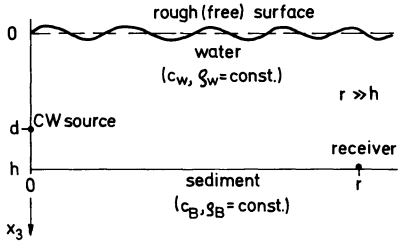

Fig. 1. Geometry of sound propagation in shallow water (2-layer fluid-fluid model)

$$\left.\begin{matrix} p^{(l)} \\ u_3^{(l)} \end{matrix}\right\} \text{ continuous at } x_3 = h \qquad (l = 1, 2, \ldots) \tag{30}$$

with,

$$\rho \frac{\partial u_3^{(l)}}{\partial t} + \frac{\partial p^{(l)}}{\partial x_3} = 0 \qquad \rho = \rho_W, \rho_B$$

= density of water layer and bottom respectively.

The wave equation for the sedimentary sea floor is

$$\frac{\partial^2 p^{(l)}}{\partial t^2} - c_B^2 \frac{\partial^2 p^{(l)}}{\partial x_i \partial x_i} = 0 \qquad \text{for } x_3 > h \tag{31}$$

c_B = sound velocity of the sea bottom.

With (29)–(31) the first-order far-field solution becomes.

$$p^{(1)}(r, x_3, t) = \sum_{n=1}^{N} r^{-\frac{1}{2}} A_n \varphi_n(x_3) \exp\{i(k_n r - \omega_0 t)\} + \text{c.c.} \tag{32}$$

with,

$$r = \sqrt{x_1^2 + x_2^2} \gg h$$

$$A_n = \frac{Q \varphi_n(d) \exp\left(i \frac{\pi}{4}\right)}{4 \rho_W \sqrt{2\pi k_n} \int_0^\infty \frac{1}{\rho} \varphi_n^2 \, dx_3}.$$

The mode functions $\varphi_n(x_3)$ and horizontal wavenumbers k_n are solutions of an eigenvalue problem. A detailed derivation of (32) is given by Kuperman and Ingenito (1977).

The acoustic field (32) only includes a finite number of trapped modes, i.e., waves which are totally reflected at the sea bottom. The continuum of leaking modes may be neglected as, due to multiple reflections, nearly all energy is transferred to the infinitely deep sea floor for long-range propagation.

To find the second-order solution, the first-order solution (32) and the representation of the surface wave-heigth (2) are inserted into the boundary condition (8) at the sea surface. Beside this the second-order wave equations of the water layer (9) and of the sedimentary halfspace (31), and the boundary conditions at the water-sediment interface (30) must be fulfilled.

For long-range propagation we only are interested in the trapped-mode portion of the solution, which becomes nonstationary (= resonant) if the scattered wavenumber and frequency satisfy the dispersion relation of trapped modes,

$$\begin{aligned} \boldsymbol{k}_s &= \boldsymbol{k}_n + s\boldsymbol{\kappa} \\ \omega_m &= \omega_0 + s\sigma \end{aligned} \qquad (s = \pm 1). \tag{33}$$

This means that ω_m ist the frequency of the mode m at the wavenumber k_s. The solution in the vicinity of the resonant branches is,

$$p^{(2)} = \sum_{\substack{\boldsymbol{k}_s \\ s=\pm 1}} r^{-\frac{1}{2}} A_n Z_{\boldsymbol{\kappa}}^s \{D_s \varphi_m(x_3) q_s(t) + \psi_s(x_3)\} \cdot \exp\{i(\boldsymbol{k}_s \boldsymbol{x} - (\omega_0 + s\sigma)t\} + \text{c.c.} \tag{34}$$

with,

$$D_s = \frac{\varphi_n'(0)\,\varphi_m'(0)}{\rho_W e_m}, \qquad e_m = \int_0^\infty \frac{1}{\rho c^2}\,\varphi_m^2\,dx_3$$

$$q_s(t) = \frac{1-\exp\{i(\omega_0 + s\sigma - \omega_m)t\}}{(\omega_0 + s\sigma)^2 - \omega_m^2}$$

where,

$$\omega_0 + s\sigma > 0 \quad \text{as} \quad \sigma \ll \omega_0.$$

At a fixed point, e.g., at the position of the receiver, the scattered field of course is stationary, but the temporal increase of the solution (34) has to be regarded along the wave path and describes the transfer of energy.

Asymptotically one obtains,

$$\lim_{t\to\infty} \frac{d}{dt} |q_s(t)|^2 = \frac{\pi}{2\omega_m^2}\,\delta(\omega_0 + s\sigma - \omega_m) \tag{35}$$

with,

$$\frac{d}{dt} = v_m \frac{\partial}{\partial r_s} \qquad (r_s \text{ parallel to } \boldsymbol{k}_s)$$

$$v_m = \frac{d\omega_m}{dk_s} \qquad \text{group velocity.}$$

We are interested in the variance spectra of X_S and Y_S from,

$$p^{(2)} = X_S \cos(\omega_0 t) + Y_S \sin(\omega_0 t). \tag{36}$$

Due to the interference pattern of the scattered modes φ_m the functions X_S and Y_S depend on the vertical coordinate x_3. It is therefore meaningful to consider the vertical average of the variance spectra.

Making use of the orthogonality of the eigenfunctions we define,

$$\frac{\rho_W c_W^2}{2h} \int_0^\infty \frac{1}{\rho c^2} (\langle X_s^2 \rangle + \langle Y_s^2 \rangle)\,dx_3 = \sum_{\boldsymbol{k}_s,\, m} E_{\boldsymbol{k}_s}^m \tag{37}$$

with,

$$\frac{\partial E_{\boldsymbol{k}_s}^m}{\partial r_s} = \frac{\pi}{2 r v_m} \sum_{\substack{n \\ s=\pm 1}} |A_n|^2 \langle |Z_{\boldsymbol{\kappa}}|^2 \rangle |D_s|^2 \frac{\rho_W c_W^2}{h} e_m\,\delta(\omega_0 + s\sigma - \omega_m).$$

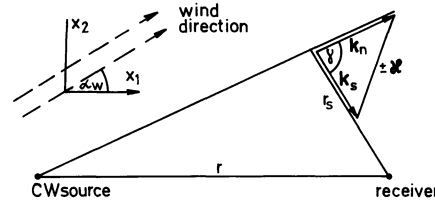

Fig. 2. Geometry of the scattering paths. $k_s = k_n + s\kappa$ ($s = \pm 1$); k: horizontal acoustic wavenumber; κ: wavenumber of surface waves

By taking care of the geometry of the scattering problem shown in Fig. 2 the integration may be carried out. Instead of discret wavenumbers a continuous notation is used and a relation between the two-dimensional acoustic and waveheight spectra is obtained. Because the measurements give only the one-dimensional acoustic spectrum, we integrate over all directions of incoming waves. The result is,

$$F_s(\sigma) = \int_{-\pi}^{\pi} \tilde{T}(\sigma, \alpha)\, E_G(\sigma, \alpha)\, d\alpha \tag{38}$$

with,

$$\tilde{T}(\sigma, \alpha) = \frac{\pi \rho_W c_W^2}{2h} \sum_{\substack{n, m \\ s = \pm 1}} \frac{e_m}{v_m^2 \omega_0^2} |A_n|^2 |D_s|^2 \frac{1}{k_n \sin^2 \gamma}.$$

More detailed investigations on wave-wave interaction are given by Hasselmann (1967), and the problem of acoustic scattering at the sea surface in shallow water is treated by Essen and Hasselmann (1970).

Ray Representation

Rays in comparison with modes stand for a further simplification of sound-propagation theory, which is obtained by neglecting the interference of up- and downwards travelling waves in the ocean. Rays are a suitable representation for a deep ocean, where adjacent modes become very close, and the (horizontal) wavenumber may be considered as a continuous variable.

The transfer function may be computed by intensity considerations. This procedure includes three steps:

(a) Determination of the radiated (1. order) intensity at each point of the sea surface: Again an isotropic point source of constant frequency is assumed [cf. (29)], and the horizontal distance from the source should be large compared with the water depth.

(b) Computation of the scattered (2. order) intensity: This can be done in dependence on the 1. order intensity with help of (11).

(c) Summarizing the intensities of all waves reaching the receiver from the different horizontal and vertical directions. The geometry is the same as in Fig. 2. As for the mode computations only the 1. and 2. order solutions are considered, which are totally reflected at the sea floor.

With the assumptions (17) about the surface-wave statistics one obtains,

$$\tilde{T}(\sigma, \alpha)=\frac{\omega_0^2 Q^2}{8\pi^2 h^2 c_W^2} \sum_{s=\pm 1} \iint \frac{\sin \vartheta_a \operatorname{tg} \vartheta_a \sin \vartheta_s \operatorname{tg} \vartheta_s}{\sin^2 \gamma} d\vartheta_a \, d\vartheta_s$$

with,

$$k_a=\frac{\omega_0}{c_W} \cos \vartheta_a; \quad k_s=\frac{\omega_s}{c_W} \cos \vartheta_s$$

$$\boldsymbol{k}_s=\boldsymbol{k}_a+s\boldsymbol{\kappa}, \quad \omega_s=\omega_0+s\sigma \approx \omega_0 \quad (s=\pm 1). \tag{39}$$

This result does not depend on the vertical positions of source and receiver, as may be understood by the outlined way of computation. In the limit of many (dense) modes the mode transfer function (38) must approach the ray transfer function (39). The summations over n and s are replaced by integrations with respect to ϑ_a and ϑ_s. Furthermore the phase change for sea-floor reflection is not considered in ray computations and (39) is obtained from (38) by assuming $\rho_B=\infty$.

Numerical Results

Before presenting computed transfer functions some general statements should be made. The equations (38), (39) show that there is no dependence on the distance between source and receiver. This surprising result follows from the geometry of the scattering problem.

The water depth is of influence on the mode transfer function as the ratio of acoustic wavelength and water depth determines the number of trapped modes.

In order to simplify the presentation of the numerical results a dimensionless transfer function is defined by [cf. (28)]

$$\Gamma(\sigma)=\frac{8\pi^2 h^2 c_W^2}{\omega_0^2 Q^2} \int_{-\pi}^{\pi} \tilde{T}(\sigma, \alpha) S_G(\sigma, \alpha) \, d\alpha. \tag{40}$$

Figure 3 shows transfer functions for continuous wavenumbers (rays) at the carrier frequencies of 200 and 400 Hz. A very strong influence of the surface-wave directions is found. Higher carrier frequencies yield a shift of the curves to higher frequencies.

It should be mentioned that the ray transfer function becomes infinite at $\gamma=\pi/2$, which refers to infinitely distant scattering points. For the frequencies regarded in our computations these points are excluded, i.e. $0 \leqq \gamma < \pi/2$.

Considering the mode-transfer function (38) it turns out that it exists of a sequence of (integrable) singularities, which result from scattering points on the straight line between source and receiver ($\gamma=0$). It is convenient to define a smoothed transfer function,

$$\Gamma_M(\sigma)=\frac{1}{2\Delta\sigma} \int_{\sigma-\Delta\sigma}^{\sigma+\Delta\sigma} \Gamma(\sigma) \, d\sigma \tag{41}$$

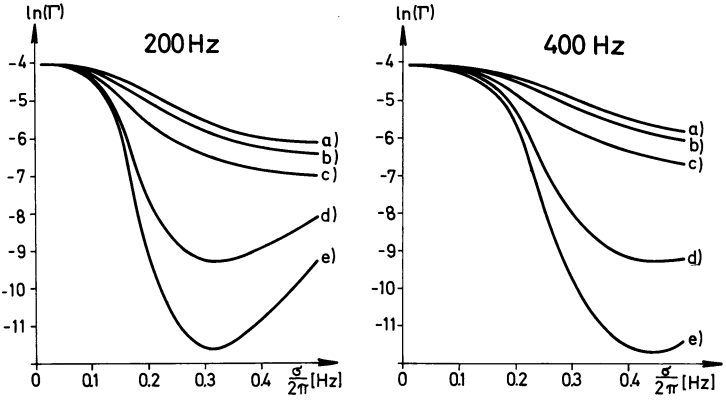

Fig. 3. Theoretical transfer functions for a ray-propagation model. CW frequencies: 200 and 400 Hz; angular-distribution functions:

$$S_G(\sigma, \alpha) = \begin{cases} \frac{1}{\pi} \hat{S}(\hat{\alpha}) & \text{for } |\hat{\alpha}| \leqq \frac{\pi}{2} \\ 0 & \text{else} \end{cases}$$

with, $\hat{\alpha} = \alpha - \alpha_W$. α_W = mean surface-wave (or wind) direction

$\hat{S}(\hat{\alpha}) = (a)\ \frac{8}{3}\cos^4\hat{\alpha}$, $(b)\ 2\cos^2\hat{\alpha}$, with, $\alpha_W = \frac{\pi}{2}$, $(c)\ \hat{\alpha}$, with, α_W = arbitrary, $(d)\ 2\cos^2\hat{\alpha}$, $(e)\ \frac{8}{3}\cos^4\hat{\alpha}$, with, $\alpha_W = 0$

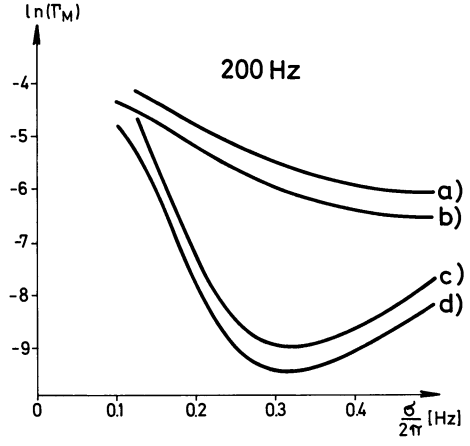

Fig. 4. Theoretical transfer functions for a mode-propagation model. CW frequency: 200 Hz; angular-distribution function:

$$S_G(\sigma, \alpha) = \begin{cases} \frac{2}{\pi} \cos(\alpha - \alpha_W) & \text{for } |\alpha - \alpha_W| \leqq \frac{\pi}{2} \\ 0 & \text{else} \end{cases}$$

water depths and mean surface-wave (or wind) directions:

$(a)\ h = 20$ m, $(b)\ h = 60$ m, with, $\alpha_W = \frac{\pi}{2}$

$(c)\ h = 20$ m, $(d)\ h = 60$ m, with, $\alpha_W = 0$;

sea-floor parameters: $c_B = 1.15 \cdot c_W$, $\rho_B = 1.9 \cdot \rho_W$

with,

$$\Delta\sigma \ll \sigma.$$

In Fig. 4 computed $\Gamma_M(\sigma)$ are shown for a carrier frequency of 200 Hz and a $\cos^2$ distribution of surface-wave directions. The water depths are 20 and 60 m, which correspond to 3 and 8 trapped modes, respectively. The low-frequency cutoff of the curves is determined by the smoothness of the function (41). For about 8 modes and

more the ray-transfer function can be used. This was verified for a number of different acoustic carrier frequencies and surface-wave direction functions.

The inverse problem, i.e., the problem to determine the 1-dimensional waveheight spectrum from the measured acoustic spectrum, requires the knowledge of the angular distribution of the surface waves. Of course this is a very crucial restriction, since the measurement of the surface-wave angular-distribution is much more difficult than the measurement of wave height. On the other hand, with the knowledge of the mean surface-wave direction and an empirical angular distribution function such as $\cos^{2\beta}(1 \leqq \beta \leqq 2)$ one may get a satisfactory estimate of the surface-wave spectrum from acoustic measurements.

The dependence of the transfer function on the surface-wave directions allows the determination of the angular distribution, provided that certain assumptions can be made. This will be discussed in the last chapter.

5. Determination of Surface-Wave Height Directions

Within several experiments in the North Sea, performed by the Institute of Geophysics in Hamburg, the acoustic and wave height spectra have been measured simultaneously, and from these data experimental transfer functions may be obtained. We will investigate the possibility of determining the directional distribution of surface waves from these data. For this purpose it must be assumed that he angular distribution S_G, cf. (27) does not depend on frequency within a certain interval,

$$S_G(\sigma, \alpha) = S_G(\alpha) \quad \text{for} \quad \sigma_\mu \leqq \sigma \leqq \sigma_0 \tag{42}$$

where,

$$\frac{\sigma_0 - \sigma_\mu}{2\pi} \approx 0.1 \text{ Hz}$$

and that the transfer function was measured for N frequencies of this interval,

$$T_n = T(\sigma_n) \quad (n = 1, \ldots, N) \tag{43}$$

with,

$$\sigma_\mu \leqq \sigma_n \leqq \sigma_0 \quad \text{(data)}.$$

The problem is now to invert the following relation, cf. (28)

$$T_n = \int_{-\pi}^{\pi} \tilde{T}(\sigma_n, \alpha)\, S_G(\alpha)\, d\alpha \tag{44}$$

where $\tilde{T}(\sigma, \alpha)$ is known from the theory presented in the preceeding chapter.

A reasonable method of inversion is a least-squares fit. In order to make use of the matrix inversion method as presented by Jackson (1972), the continuous distribution function is approximated by a number of discret steps,

$$S_G(\alpha) + S_G(\alpha + \pi) = S_m \quad \text{for} \quad (m-1) \cdot \Delta\alpha - \frac{\pi}{2} \leqq \alpha \leqq m \cdot \Delta\alpha - \frac{\pi}{2} \tag{45}$$

with,

$$\Delta\alpha=\frac{\pi}{M}\ (m=1, \ldots, M) \qquad \text{(model)}.$$

Ocean surface waves travelling in opposite directions yield the same contribution to the transfer function. This ambiguity has been taken into consideration by defining S_m in (45).

With (45) the inversion problem (44) becomes,

$$T_n=\sum_{m=1}^{M} G_{nm}\cdot S_m \tag{46}$$

with,

$$G_{nm}=\int_{(m-1)\cdot\Delta\alpha-\frac{\pi}{2}}^{m\cdot\Delta\alpha-\frac{\pi}{2}} \tilde{T}(\sigma_n, \alpha)\, d\alpha.$$

The data T_n depend linearly on the model parameter S_m. We assume that the number of data exceeds the number of model parameters,

$$N>M. \tag{47}$$

Following Jackson (1972) we consider the coupled eigenvalue problem,

$$\begin{aligned} G\,v &= \lambda\mu \\ G^T u &= \lambda v \end{aligned} \tag{48}$$

where G is the $n\times m$ matrix defined by (46), and u and v are eigenvectors with n or m components, respectively. The nonzero eigenvalues are computed and ranked in decreasing order of magnitude.

$$\lambda_1^2\geqq\lambda_2^2\geqq\ldots\geqq\lambda_p^2>0 \tag{49}$$

with,

$$p\leqq M<N.$$

The generalized (Lanczos) inverse of G is defined by,

$$H=V\Lambda^{-1}U^T \tag{50}$$

where U and V are the $n\times p$ and $m\times p$ eigenvector matrices, respectively, and Λ is the diagonal $p\times p$ matrix of the nonzero eigenvalues. It can be shown that H is a least-aquares inverse.

In order to test the method, angular distribution functions have been computed for artificial data. In Fig. 5 an example is shown, where the data correspond to a $\cos^2$ angular distribution with two different main directions. The number of data is $N=11$ from the frequency interval 0.1–0.2 Hz, and the number of model parameters is $M=5$ or $M=7$. The number of nonzero eigenvalues is M, but the higher eigenvalues become very small. It is useful to construct the inverse H out of

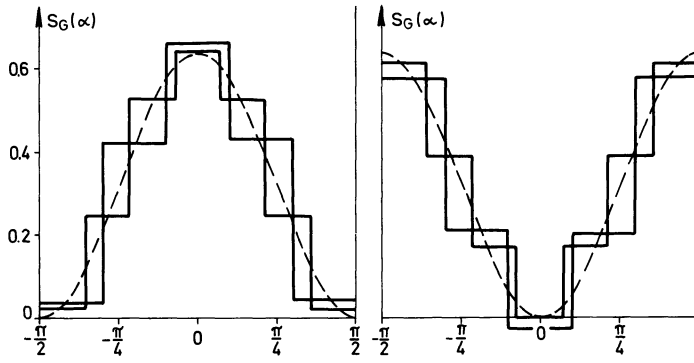

Fig. 5. Angular-distribution functions computed by matrix inversion from theoretical "data". CW frequency: 200 Hz; N = 11 data, i.e., computed values of the transfer function at equidistant frequencies between 0.1 and 0,2 Hz and for continuous angular-distribution functions *(dashed lines)*; M = 5,7 model parameters, respectively

eigenvectors only, that correspond to the p largest eigenvalues, which are in our example, $p=3$ for $M=5$, and $p=5$ for $M=7$.

As may be expected for artificial data the steps of the model angular distribution S_m fit the continuous $\cos^2$ distribution quite well. Measured data and an estimation of errors will be presented in a later paper.

Acknowledgements. This research was supported by the "Sonderforschungsbereich 94, Meeresforschung Hamburg".

References

Barrick, D.E., Evans, H.W., Weber, B.L.: Ocean surface currents mapped by Radar, Science **198**, 138–144, 1977

Clark, J.G., Kronengold, M.: Long-period fluctuations of CW signals in deep and shallow water. J. Acoust. Soc. Am. **56**, 1071–1083, 1974

Essen, H.-H.: Wave-facet interaction model applied to acoustic scattering from a rough sea surface, Acustica **31**, 107–113, 1974

Essen, H.-H., Hasselmann, K.: Scattering of low-frequency sound in the ocean, Z. Geophys. **36**, 655–678, 1970

Essen, H.-H., Schirmer, F., Siebert, J.: Measurements of ocean surface-waves with an acoustic range. Dt. hydrogr. Z. **31**, 7–15, 1978

Hasselmann, K.: Nonlinear interactions treated by the methods of theoretical physics (with application to the generation of waves by wind). Proc. Roy. Soc. A **299**, 77–100, 1967

Jackson, D.D.: Interpretation of inaccurate, insufficient and inconsistent data. Geophys. J.R. Astron. Soc. **28**, 97–109, 1972

Kinsman, B.: Wind waves – their generation and propagation on the ocean surface. Prentice-Hall, Englewood Cliffs, 1965

Kuperman, W.A., Ingenito, F.: Attenuation of the coherent component of sound propagating in shallow water with rough boundaries. J. Acoust. Soc. Am. **61**, 1178–1187, 1977

Rice, S.O.: Mathematical analysis of random noise, from Wax: Selected papers on noise and stochastic processes. Dover, New York 1954

Tyler, G.L., Teague, C.C., Stewart, R.H., Peterson, A.M., Munk, W.H., Joy, J.W.: Wave directional spectra from synthetic aperture observations of radio scatter. Deep-Sea Res. **21**, 989–1016, 1974

Received July 31, 1978; Accepted January 12, 1979